Scientific Research Publishing

Journal of Biosciences and Medicines, 2025, 13(2), 243-255
https://www.scirp.org/journal/jbm
ISSN Online: 2327-509X
ISSN Print: 2327-5081

Suppression of Cell Traction Force and Enhanced Force Polarity are Key Factors in Vascular Smooth Muscle Cell Differentiation Induced by Low Serum Culture

Kazuaki Nagayama, Harunobu Tatsuno

Micro-Nano Biomechanics Laboratory, Department of Mechanical Systems Engineering, Ibaraki University, Ibaraki, Japan
Email: kazuaki.nagayama.bio@vc.ibaraki.ac.jp

How to cite this paper: Nagayama, K. and Tatsuno, H. (2025) Suppression of Cell Traction Force and Enhanced Force Polarity are Key Factors in Vascular Smooth Muscle Cell Differentiation Induced by Low Serum Culture. *Journal of Biosciences and Medicines*, **13**, 243-255.
https://doi.org/10.4236/jbm.2025.132019

Received: January 7, 2025
Accepted: February 15, 2025
Published: February 18, 2025

Abstract

Vascular smooth muscle cells (VSMCs) in the arterial walls play important roles in regulating vascular contraction and dilation. VSMCs actively remodel the arterial walls and dedifferentiate from the contractile to the synthetic phenotype under pathological conditions. The mechanism underlying phenotypic transition of VSMCs is important for understanding its role in the pathophysiology of disease. Although numerous studies have reported various biochemical pathways that stimulate the phenotypic transition of VSMCs, very little is known about relation between their phenotypic transition and cellular traction force, which affects many cellular functions. In this study, we induced the differentiation of cultured VSMCs from the synthetic to the contractile phenotype by a low-serum cultivation and investigated changes in the cell traction forces using traction force microscopy technique. The expression of α-SMA, a contractile phenotype marker protein, was significantly upregulated with maturation of actin stress fibers in the low-serum culture, indicating VSMC differentiation was promoted in our experiments. The cells changed their morphology to an elongated bipolar shape, and the direction of the cell traction forces tended to align in the direction of the cell's major axis. Despite the promotion of contractile differentiation in VSMCs, the overall cell traction forces were significantly reduced, indicating that excessive cell mechanical tension, which might induce cell proliferation and migration, was suppressed during contractile differentiation. These results suggest that suppression of cell traction force and enhanced force polarity might be key factors in VSMC differentiation induced by low serum culture.

Keywords

Cell Biomechanics, Mechanobiology, Phenotype, Cytoskeleton, Traction

Force Microscopy

1. Introduction

Vascular smooth muscle cells (VSMCs) regulate the vascular contraction and dilation [1]. They actively remodel the vascular wall in which they reside through biochemical and biomechanical signals [2] [3]. VSMCs maintain the mechanical hoop stress in the wall to a physiological level through their contractility [4]. In normal vascular walls, mature differentiated VSMCs have a contractile phenotype. Contractile VSMCs have a bipolar elongated morphology and remain quiescent in proliferation and metabolism of extracellular matrix (ECM). Contractile VSMCs express a unique repertoire of contractile proteins, agonist receptors, and ion channels [5] [6]. Under pathological conditions, such as hypertension and atherogenesis VSMCs undergo dedifferentiation from the contractile phenotype to the synthetic phenotype. Synthetic VSMCs exhibit a stellate shape, express fewer contractile proteins, and are active during proliferation, migration, and ECM turnover [7]. A similar change in cell dedifferentiation is observed when VSMCs are removed from the native aortic tissue and grown in culture conditions. VSMCs exhibit a less elongated morphology and spread randomly on the flat surface of the culture dishes. The mechanism underlying the differentiation and dedifferentiation of VSMCs is important for vascular adaptation and repair as well as the pathophysiology of diseases. Additionally, understanding the differentiation and dedifferentiation mechanisms of VSMCs can aid in developing tissue-engineered blood vessels.

Previous studies have investigated the effect of biochemical factors on phenotypic transition of VSMCs. Reactive oxygen species promote VSMC differentiation through MAP kinase-dependent pathway [8] and serum response factors regulate the phenotypic switching of VSMCs [9]. Serum starvation culture medium containing cell survival factors, such as insulin and transferrin, also induces VSMC differentiation from the synthetic to the contractile phenotype [10]. Additionally, the serum starvation culture restored contractile protein expression to the levels of freshly isolated contractile VSMCs [11]. Although several studies have reported the biochemical factors involved in the stimulation of VSMC phenotypic transition, limited information is available about relation between their phenotypic transition and cellular traction forces, which may affect many cellular functions, such as cell migration [12] [13] and proliferation [14] [15] as well as the pathological conditions [16].

Thus, in this study, we induced the differentiation of cultured VSMCs from the synthetic to the contractile phenotype by a low-serum culture condition and investigated changes in the cell morphology and intracellular traction forces by using the fluorescent microscopy imaging analysis and traction force microscopy technique.

2. Materials and Methods

2.1. Cell Culture and Induction of VSMC Differentiation

A7r5 rat embryonic aortic smooth muscle cell lines (VSMCs; CRL-1444, ATCC, USA) were used as the test model. The VSMCs were cultured in a standard culture proliferative medium, which was Dulbecco's modified Eagle's medium (DMEM, Wako) supplemented with 10% fetal bovine serum (FBS, JRH Bioscience, USA), penicillin (100 U/mL), and streptomycin (100 mg/mL) (Sigma) at 37˚C in 5% CO_2 and 95% air. The cells were passaged repeatedly at a 1:4 split ratio when they reached approximately 80% confluency. The VSMCs were induced to undergo phenotypic transition from the synthetic state to the contractile state using a low-serum medium, which was DMEM supplemented with 0.5% FBS. After the VSMCs reached approximately 70% confluency in the proliferative medium, the culture medium was replaced with the low-serum medium. The cells were then cultured in the low-serum medium for 7 days to induce VSMC differentiation.

2.2. Cell Staining

To assess VSMC differentiation of cells, major smooth muscle contractile differentiation proteins (α-SMA, Transgelin, and F-actin) and nuclei were subjected to fluorescence staining. VSMCs were fixed with phosphate-buffered saline (PBS (−), Nissui, Tokyo, Japan) containing 3.7% formaldehyde for 10 min. The cells were permeabilized with PBS (−), containing 0.1% Triton X-100 (ICN Biomedicals, Irvine, CA, USA), for 5 min. Next, the cells were rinsed with PBS (−) containing 1% bovine serum albumin (BSA) to block the nonspecific protein binding. The fixed cells were incubated with the blocking solution for 30 min before treatment with staining reagents. The samples were incubated with mouse antibodies against α-SMA (1:200 dilution, A2547, clone 1A4, Sigma) or transgelin (1:200 dilution, ab14106, abcam) for 60 min at room temperature (25˚C). The samples were then incubated with the secondary antibody (rabbit anti-mouse Alexa Fluor 488, 1:200 dilution, Invitrogen) for 60 min at room temperature. All antibodies were diluted in PBS (−) containing 1% BSA. The cells were stained with 200 nM Alexa Fluor 546-conjugated phalloidin (Molecular Probes, Eugene, OR, USA) for 60 min to stain the F-actin cytoskeleton. The nucleus was visualized by staining the intranuclear DNA with Hoechst 33342 (Invitrogen, Carlsbad, CA, USA) for 30 min.

2.3. Analysis of Cell Morphology and VSMC Differentiation

The fluorescent image of the stained cells was captured using an inverted fluorescence microscope (IX71, Olympus, Japan) equipped with an electron-multiplying charge-coupled device (EM-CCD) camera (C9100-12, Hamamatsu Photonics, Japan), light-emitting diode (LED) light source (X-Cite XLED1, Olympus), and a 20X objective lens (numerical aperture = 0.40). Optical components of the microscope, such as LED light source intensity, filters and iris diaphragms were kept under the same condition during the measurements.

The cell area (A_{cell}), shape index (SI_{cell}), and aspect ratio (AR_{cell} = major axis length/minor axis length) were measured from additional projection images. *SI* expressed by Equation (1), is defined as 1.0 for a circle and approaches zero for highly elongated shapes.

$$SI_{cell} = \frac{4\pi A}{P^2} \tag{1}$$

where A and P are the projected area and perimeter of the nucleus, respectively.

The mean fluorescence intensity of F-actin cytoskeleton (I_{actin}), α-SMA (I_{SMA}), and transgelin (I_{Trans}) was measured and the intensity ratio of α-SMA to F-actin I_{SMA}/I_{actin} and the intensity ratio of transgelin to F-actin, I_{Trans}/I_{actin} were examined as indices of VSMC differentiation.

2.4. Fabrication of PA Gel for Cell Traction Force Microscopy

Polyacrylamide (PA) gel substrates were fabricated as described previously [17]. Briefly, PA gel solutions can be prepared by mixing a 40% acrylamide solution (40% Acrylamide, BIO-RAD) with a cross-linking agent, 40%T-5%C (%T, total monomer concentration; %C, cross-linking density) acrylamide-Bis solution (40% Acrylamide/Bis solution 19:1, BIO-RAD) can be prepared by mixing the above mixture with distilled water. In this study, the above mixture was diluted with distilled water to the desired concentration and two thermal polymerization accelerators (TEMED, and APS, BIO-RAD) were added. The solution was dropped onto a 35-mm glass-bottom culture dishes (No. 0, Matsunami, Osaka, Japan), covered with a cover glass (18 mm on each side) to make the gel surface uniform, and placed in an incubator (SCA-165DS, Astec) maintained at 37˚C for 30 min for gelation. The upper cover glass was then removed, and the surface of the substrates was coated with a thin layer of the same PA gel solution containing fluorescently labeled microparticles (FluoSpheres®, diameter 0.2 μm, F8811, Thermo Fisher Scientific). Then, the PA gel substrates were washed with buffer solution HEPES, and stored at 4˚C, and shielded from light until following experiments.

To determine the elastic modulus of PA gel substrates, atomic force microscopy (AFM) indentation measurements were performed using a NanoWizard IV AFM (JPK Instruments-AG, Germany) mounted on top of an inverted optical microscope (IX73, Olympus, Japan) equipped with a digital CMOS camera (Zyla, Andor). For AFM indentation measurements, we used the pyramidal tip of V-shaped silicon nitride cantilevers, equipped with a 5 μm borosilicate bead (CP-PNPS-BSG-A, sQube). The spring constant of each cantilever was determined before measurements, using the thermal noise method (Hutter and Bechhoefer, 1993), in water. The tip of the cantilever was placed over the PA gels or PDMS substrates and monitored using the optical microscope. Indentations were performed at 10 different points in each substrate with a constant indentation speed of 2 μm/s. Substrate elasticity values were calculated from the force-indentation curves by applying a Hertzian model [18] for spherical tips, assuming the sample is isotropic and linearly elastic.

$$F = \frac{4}{3}\frac{E_{sub}}{\left(1-\upsilon^2\right)}R^{\frac{1}{2}}\delta^{\frac{3}{2}} \quad (2)$$

where F is the applied force, E_{sub} is the elastic modulus of substrates, ν is the Poisson's ratio (0.5 for a non-compressible sample), R is the radius of the beads of the cantilever tip, and δ is the indentation depth of PA gel recorded in the force curves. The elastic modulus of the fabricated PA gels was E_{sub} = 9.45 ± 0.29 kPa (10 substrates), which is comparable to the elastic modulus of substrate in previous studies on vascular smooth muscle cell differentiation.

2.5. Imaging for Traction Force Microscopy

For sample preparation, PA gel substrates were first incubated at room temperature for 4 h with a solution of 20 μg/mL fibronectin (F1141, Sigma) and then washed with PBS. Before cell seeding, the substrates were washed with sterile PBS (−). Only those PA gel substrates that had a homogeneous distribution of the microparticles were selected for cell seeding.

VSMCs cultured in the proliferative medium (control group) or in the low-serum medium (low-serum group) were detached from the culture dishes and then seeded on the PA gel substrates and allowed to reattach to the substrate for 24 h (**Figure 1(A)**). Before the traction force microscopy experiments, cell plasma membranes were fluorescently stained using CellMaskTM Orange (C10045, Invitrogen) in accordance with the previous study [19], and washed with PBS (−).

The specimen cells were mounted on the stage of the inverted fluorescence microscope equipped with cell culture incubator (Stage top incubator, Tokai Hit, Japan) and maintained at 37˚C in 5% CO_2 and 95% air. Differential interference contrast (DIC) microscope images of VSMCs on the PA gel substrate (**Figure 1(B)**) and the fluorescence image of cell membrane (**Figure 1(C)**) were captured by the EM-CCD camera using a 40× objective (UPLSAPO 40 × 2, NA = 0.95, Olympus). When cells attach and pull on the substrate they generate traction forces on the substrate, displacing the particles from their original position (**Figure 1(D)**). When the cells are detached (adding trypsin), the particles return to their original position due to the elastic properties of the substrate (**Figure 1(E)**). Thus, images of the particles are taken before and after removing the cells and merging (**Figure 1(F)**, **Figure 1(G)**).

2.6. Analysis of Cellular Traction Forces

The displacement vectors of the surface of PA gel substrates generated by the cellular traction forces were obtained by the particle image velocimetry (PIV) method by comparing the images of the fluorescence particles embedded in the PA gel substrates before and after cell detachment. The displacement vectors were measured by iterative PIV, a plug-in for ImageJ developed by Tseng *et al.* [20]. The displacement vectors and the average elastic modulus of the substrate obtained in 2.3 were used to obtain the traction stress vectors derived from the cell traction forces by Fourier transform traction cytometry (FTTC), a plug-in developed

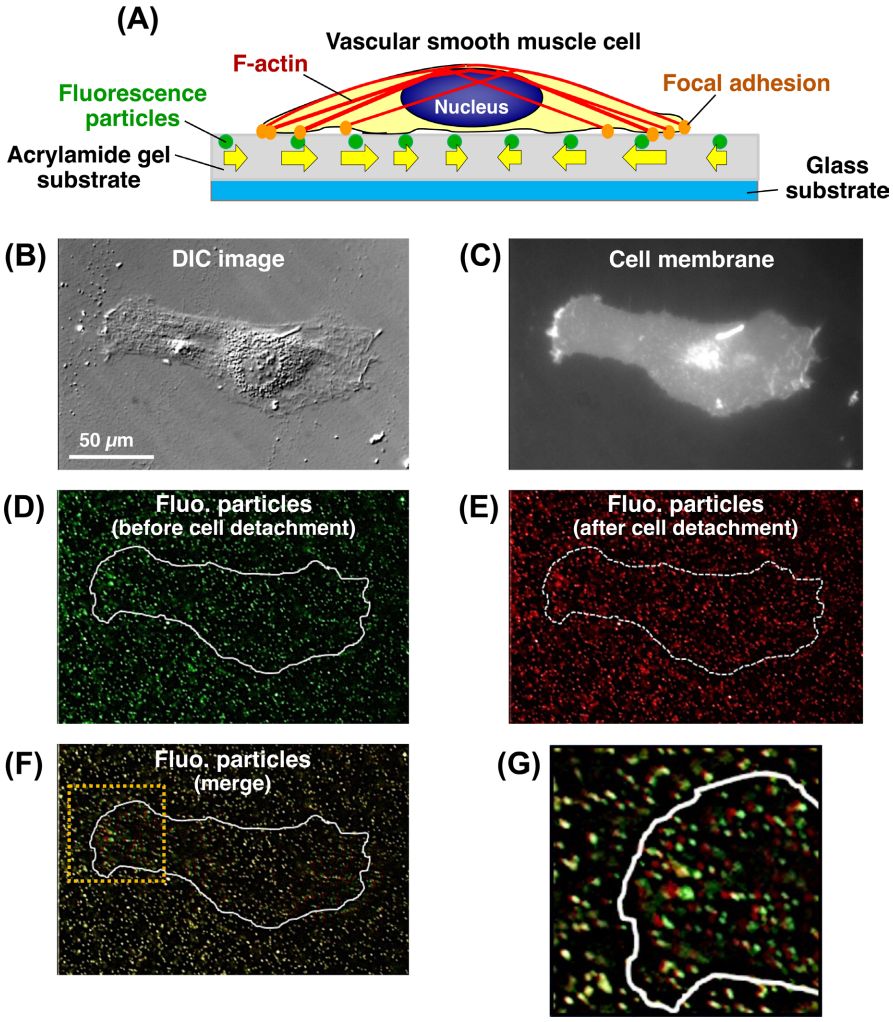

Figure 1. Diagram of traction force microscopy experiments. Vascular smooth muscle cells (VSMCs) are seeded on elastic substrates (polyacrylamide (PA) gel) that contain fluorescent particles on the top (A). Differential interference contrast (DIC) microscope image of VSMC on the PA gel substrate (B) and the fluorescence image of its membrane to capture its outline (C). When cells attach and pull on the substrate they generate traction forces on the substrate, displacing the particles from their original position (D). When the cells are detached (adding trypsin), the particles return to their original position due to the elastic properties of the substrate (E). Thus, images of the particles are taken before and after removing the cells and merging (F). A magnification of the dashed square region in F (G).

by Butler *et al.* [21]. The total cell traction force was calculated by multiplying the average value of the cell major-axis component of traction stress vectors and cell half area.

2.7. Statistical Analysis

Data are expressed as means ± standard deviation (SD). Statistical significance was assessed using the student's paired and unpaired *t*-test with the statistical analysis program MEPHAS (https://alain003.phs.osaka-u.ac.jp/mephas/). A significance level of $P < 0.05$ and $P < 0.01$ was used for all analyses.

3. Results and Discussion

The changes in the cell morphology and contractile protein distribution and expression during low-serum culture were evaluated using fluorescent imaging (Figure 2). VSMCs cultured in both proliferative medium (control group) and the low-serum medium (low-serum group) sufficiently spread on the dishes (Figure 2(A), Figure 2(D)) and exhibited thick bundles of actin stress fibers especially

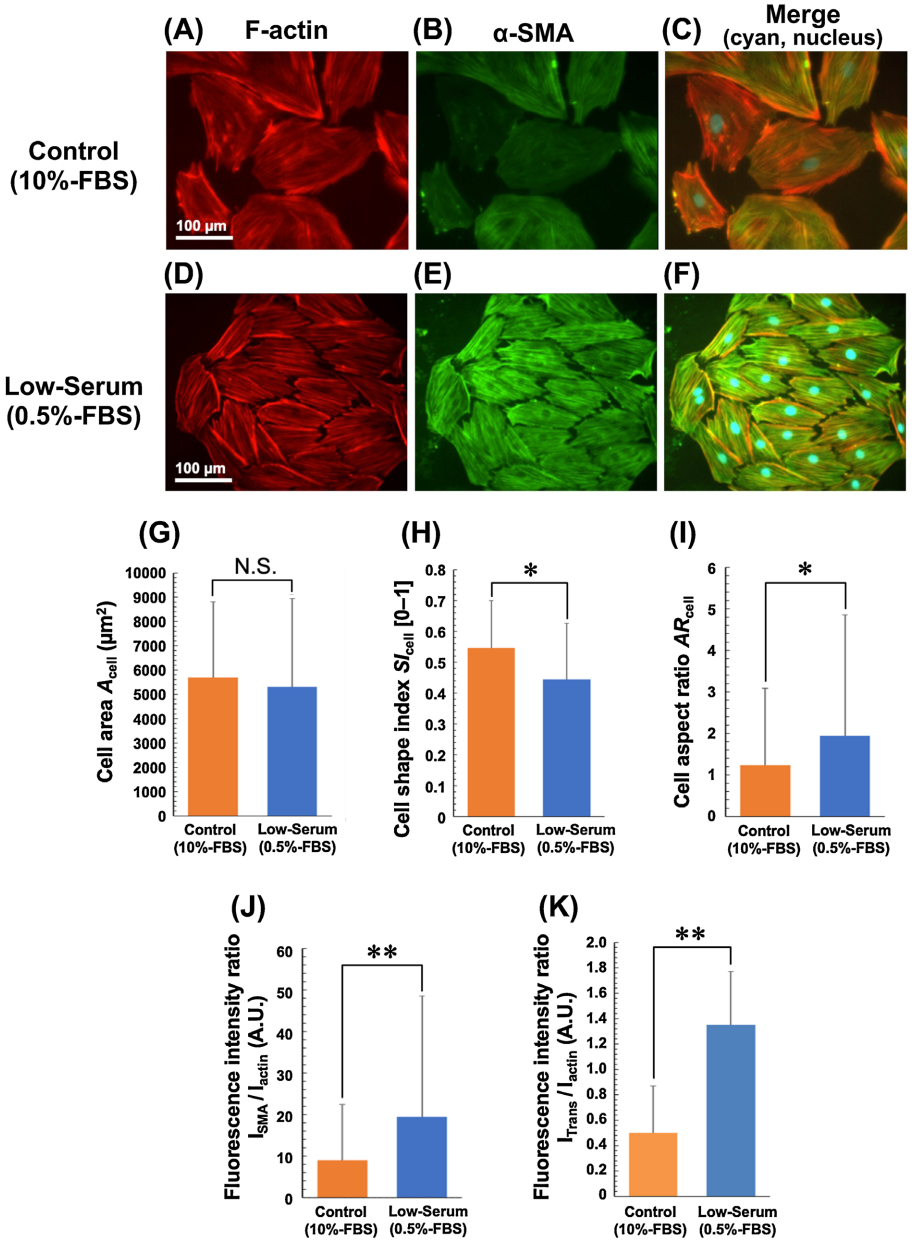

Figure 2. Representative fluorescent images of the actin cytoskeleton (red) and *α*-SMA (green) of vascular smooth muscle cells (VSMCs) cultured in standard culture proliferative medium (A)-(C) and low-serum medium (D)-(F). Changes in cell area A_{cell} (G), cell shape index SI_{cell} (H), cell aspect ratio AR_{cell} (I), and fluorescence intensity ration of *α*-SMA to F-actin I_{SMA}/I_{actin} (J) and intensity ration of transgelin to F-actin I_{Trans}/I_{actin} (K). Over 100 cells in 4 dishes were analyzed in each group. Mean + SD. (*): $P < 0.05$. (**): $P < 0.01$.

in the low-serum group (**Figure 2(D)**). VSMCs in control group exhibited weak α-SMA fluorescence and the expression level of α-SMA varied in each cell (**Figure 2(B)**, **Figure 2(C)**), which indicated the low contractility and synthetic phenotype. Contrastingly, thick bundles of α-SMA colocalized on the F-actin fluorescence were clearly observed in the low-serum group (**Figure 2(E)**, **Figure 2(F)**). Although no significant difference was observed in the cell area of both groups (**Figure 2(G)**), the cell shape index SI_{cell} was smaller in the low serum group (**Figure 2(H)**) and cell aspect ratio was larger in the low serum group (**Figure 2(I)**), indicating that the VSMCs changed to an elongated morphology. The fluorescence intensity ratio of α-SMA to F-actin and the intensity ratio of transgelin to F-actin significantly increased in low-serum group (**Figure 2(J)**, **Figure 2(K)**), which indicates that culturing the cells in low-serum medium promotes VSMC contractile differentiation.

Previous studies have reported that the major contractile markers, α-SMA and calponin of VSMCs increased markedly when cultured in serum-free medium [8] [22]. The expression levels of these markers were statistically similar to those of the freshly isolated VSMCs from aortic tissue [11], which concurred with the results of our study. Piludu *et al.* [23] demonstrated that thymosin β4, a potent inhibitor of actin polymerization, translocated from the cytoplasm into the cell nucleus under serum starvation conditions. Pavlyk *et al.* [24] also reported that the dynamic actin concentrated at the leading edge of cells cultured in the serum containing medium, but it disappeared with the inhibition of cell migration after serum starvation. These previous reports indicated that low-serum stimulation inhibits the actin dynamics in cells and stabilizes the filamentous structures of actin cytoskeleton. This may facilitate F-actin maturation observed in the low-serum group in our study. Such F-actin stabilization may promote α-SMA contractile actin isoform, resulting in sufficient contractile differentiation.

Next, the magnitude and distribution of intracellular traction forces were analyzed for the VSMCs in the control and low serum groups by traction force microscopy (**Figure 3**). Cells in the control group were polygonal in shape (**Figure 3(A)**), while those in the low serum group were elongated (**Figure 3(D)**). In both groups of cells, traction forces were generated toward the center of the cell, and the PA gel substrate deformed significantly at the cell periphery (**Figure 3(B)**, **Figure 3(E)**, arrows), and mechanical polarity was observed in the direction of traction stresses (**Figure 3(C)**, **Figure 3(F)**). This indicates that the cells maintain their morphology by generating the same amount of force at both ends of the cells and maintaining mechanical balances.

Finally, the results obtained by traction force microscopy (**Figure 3**) were analyzed to quantify the cell total traction forces (**Figure 4**). The average total traction force of VSMCs in the control group was approximately 400 nN, which is on the same order of magnitude as that measured using the elastic micropillar technique in our previous study [25]. Interestingly, the total traction force in the low-serum group was dramatically reduced to a quarter of that in the control group (**Figure 4(A)**),

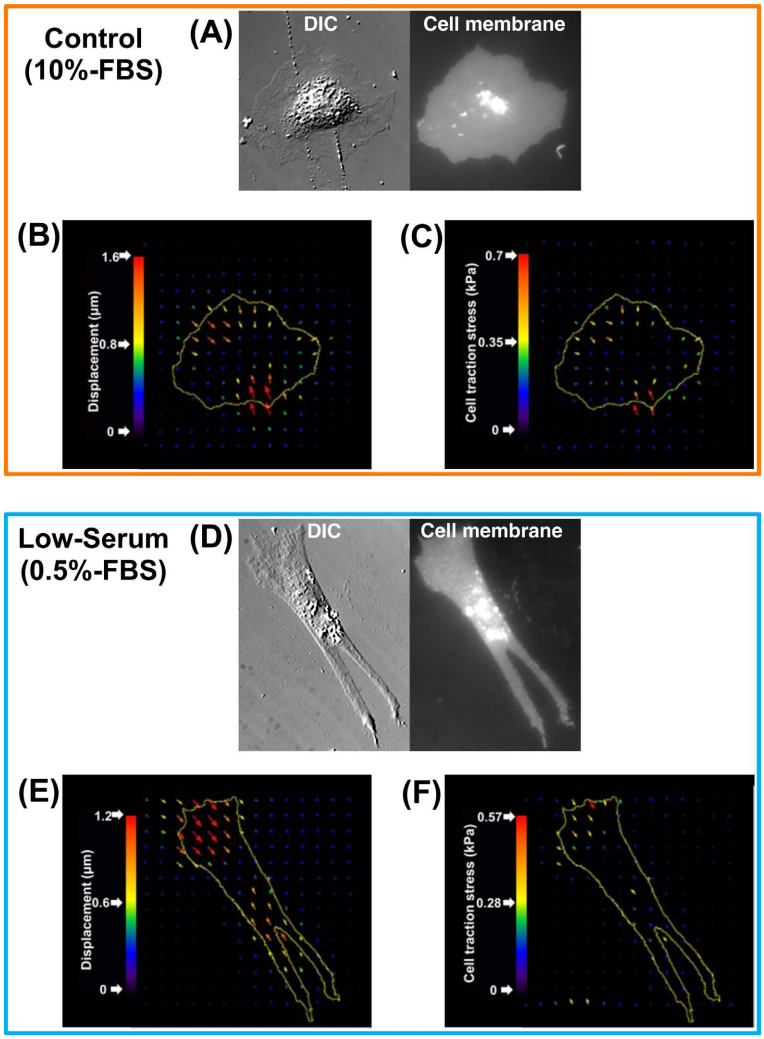

Figure 3. Differential interference contrast (DIC) microscope image of VSMC on the PA gel substrate and the fluorescence image of its membrane to capture its outline (A), (D). Representative substrate displacement maps (B), (E) and traction stress maps (C), (F) of VSMCs in the control (B), (C) and the low-serum groups (E), (F).

even though they significantly differentiated to contractile phenotype in the low-serum condition. Analysis of the direction of the traction force vectors in the cells revealed that the direction of the force vector was relatively random in the control cells (**Figure 4(B)**, orange bars), whereas in the low-serum group, the force vector was significantly aligned in the major axis direction of the cells (**Figure 4(B)**, blue bars) with significant contractile differentiation.

VSMCs in actual vascular tissue are elongated in morphology and have a contractile phenotype. Previous reports demonstrated that VSMCs freshly isolated from vascular tissue have a contractile phenotype and have significantly stiffer characteristics than cells that have become synthetic phenotype in culture [26] [27]. Thus, it has been thought that intracellular mechanical tension is also higher in VSMCs with contractile phenotype. On the other hand, other reports suggest that enhancement of cell mechanical tension due to actomyosin activation does

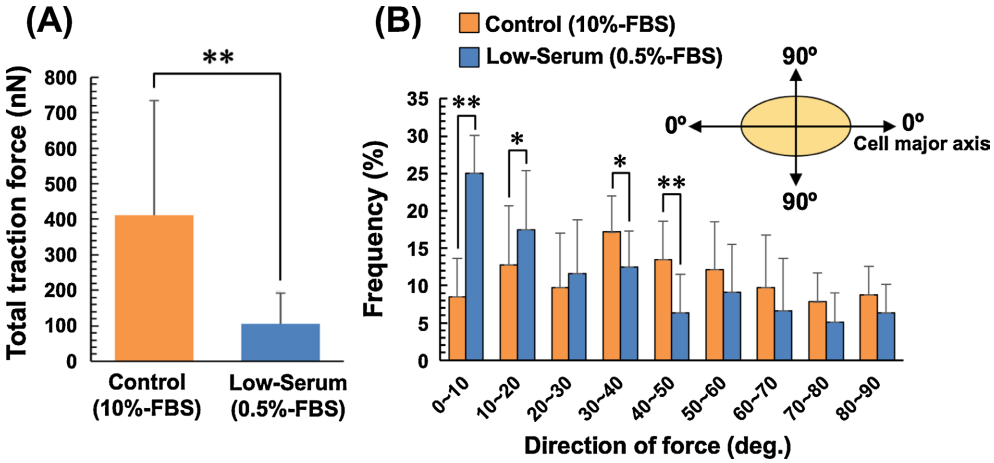

Figure 4. Changes in the total traction forces (A) and the direction of the intracellular traction forces (B) in VSMCs following the low-serum culture. Mean + SD. (*): $P < 0.05$. (**): $P < 0.01$.

not necessarily for VSMC differentiation to contractile phenotype: VSMCs cultured on the substrates of medium stiffness (E_{sub} = −40 kPa) became elongated (polarized) morphology with enhancement of contractile protein expression while their intracellular mechanical tension was reduced [17]. It has also been reported that VSMC motility is enhanced with relatively high intracellular tension and diverse actin fiber orientations [25]. Furthermore, Yamashiro *et al.* [28] found that when VSMCs are mechanically stimulated at their focal adhesion sites, a matricellular protein, thrombospondin-1 (Thb1), binds to integrins and localizes to the focal adhesions of VSMCs, inducing nuclear shuttling of a transcriptional coactivator, Yes-associated protein (YAP), and promoting proliferation and dedifferentiation of VSMCs. Considering the above, the following mechanisms are possible cell differentiation responses observed in this study: The reduction of serum concentrations in the low-serum cultivation put VSMCs in a "standby state", suppressing the activation of the actomyosin contractile machinery and the formation of focal adhesions, which may have led to the fusion and stabilization of actin stress fibers anchoring at the limited focal adhesion, inducing elongation and polarization of the cell shape and VSMC differentiation.

In conclusion, we induced the differentiation of cultured VSMCs from the synthetic to the contractile state by the low-serum cultivation and investigated changes in the cell traction forces using traction force microscopy technique. The cells in the low-serum group increased α-SMA expression ratio and changed their morphology elongated bipolar shape, and the direction of their traction forces tended to align in the direction of the cell's major axis. Despite the promotion of contractile differentiation, the overall cell traction forces were significantly reduced. These results suggest that suppression of cell traction force and enhanced force polarity might be key factors in VSMC differentiation induced by low serum culture.

Acknowledgements

This work was supported in part by a Grant-in-Aid from the Ministry of Education,

Culture, Sports, Science, and Technology, Japan (nos. 21H03804, 22K19890, and 24K03246).

Conflicts of Interest

The authors declare no conflicts of interest regarding the publication of this paper.

References

[1] Wolinsky, H. (1972) Long-Term Effects of Hypertension on the Rat Aortic Wall and Relation to Concurrent Aging Changes. *Circulation Research*, **30**, 301-309. https://doi.org/10.1161/01.RES.30.3.301

[2] Hansen, T.R., Dineen, D.X. and Pullen, G.L. (1980) Orientation of Arterial Smooth Muscle and Strength of Contraction of Aortic Strips from DOCA-Hypertensive Rats. *Blood Vessels*, **17**, 302-311. https://doi.org/10.1159/000158261

[3] Matsumoto, T. and Hayashi, K. (1996) Stress and Strain Distributions in Hypertensive and Normotensive Rat Aorta Considering Residual Strain. *Journal of Biomechanical Engineering*, **118**, 62-73. https://doi.org/10.1115/1.2795947

[4] Matsumoto, T., Tsuchida, M. and Sato, M. (1996) Change in Intramural Strain Distribution in Rat Aorta Due to Smooth Muscle Contraction/Relaxation. *American Journal of Physiology*, **271**, 1711-1716. https://doi.org/10.1152/ajpheart.1996.271.4.H1711

[5] Campbell G. and Campbell J. (1995) The Vascular Smooth Muscle. Schwartz, S. and Mecham, R., Eds., *Academic Press*, 503-522.

[6] Hao, H., Gabbiani, G., Camenzind, E., Bacchetta, M., Virmani, R. and Bochaton-Piallat, M.L. (2006) Phenotypic Modulation of Intima and Media Smooth Muscle Cells in Fatal Cases of Coronary Artery Lesion. *Arteriosclerosis, Thrombosis & Vascular Biology*, **26**, 326-332. https://doi.org/10.1161/01.ATV.0000199393.74656.4c

[7] Kocher, O., Gabbiani, F., Gabbiani, G., Reidy, M.A., Cokay, M.S. and Peters, H. (1991) Phenotypic Features of Smooth Muscle Cells during the Evolution of Experimental Carotid Artery Intimal Thickening. Biochemical and Morphologic Studies. *Laboratory Investigation*, **65**, 459-470.

[8] Su, B., Mitra, S., Gregg, H., Flavahan, S., Chotani, M.A., Clark, K.R., Goldschmidt-Clermont, P.J. and Flavahan, N.A. (2001) Redox Regulation of Vascular Smooth Muscle Cell Differentiation. *Circulation Research*, **89**, 39-46. https://doi.org/10.1161/hh1301.093615

[9] Lee, M.Y., Park, C., Ha, S.E., Park, P.J., Berent, R.M., Jorgensen, B.G., Corrigan, R.D., Grainger, N., Blair, P.J., Slivano, O.J., Miano, J.M., Ward, S.M., Smith, T.K., Sanders, K.M. and Ro, S. (2017) Serum Response Factor Regulates Smooth Muscle Contractility via Myotonic Dystrophy Protein Kinases and L-Type Calcium Channels. *PLOS ONE*, **12**, e0171262. https://doi.org/10.1371/journal.pone.0171262

[10] Lavender, M.D., Pang, Z., Wallace, C.S., Niklason, L.E. and Truskey, G.A. (2005) A System for the Direct Co-Culture of Endothelium on Smooth Muscle Cells. *Biomaterials*, **26**, 4642-4653. https://doi.org/10.1016/j.biomaterials.2004.11.045

[11] Sakamoto, N., Kiuchi, T. and Sato, M. (2011) Development of an Endothelial-Smooth Muscle Cell Coculture Model Using Phenotype-Controlled Smooth Muscle Cells. *Annals of Biomedical Engineering*, **39**, 2750-2758. https://doi.org/10.1007/s10439-011-0372-8

[12] Renkawitz, J., Kopf, A., Stopp, J., de Vries, I., Driscoll, M.K., Merrin, J., Hauschild,

R., Welf, E.S., Danuser, G., Fiolka, R. and Sixt, M. (2019) Nuclear Positioning Facilitates Amoeboid Migration along the Path of Least Resistance. *Nature*, **568**, 546-550. https://doi.org/10.1038/s41586-019-1087-5

[13] Woychek, A. and Jones, J.C.R. (2019) Nesprin-2G Knockout Fibroblasts Exhibit Reduced Migration, Changes in Focal Adhesion Composition, and Reduced Ability to Generate Traction Forces. *Cytoskeleton* (*Hoboken*), **76**, 200-208. https://doi.org/10.1002/cm.21515

[14] Versaevel, M., Grevesse, T. and Gabriele, S. (2012) Spatial Coordination between Cell and Nuclear Shape within Micropatterned Endothelial Cells. *Nature Communications*, **3**, Article No. 671. https://doi.org/10.1038/ncomms1668

[15] Nagayama, K., Hamaji, Y., Sato, Y. and Matsumoto, T. (2015) Mechanical Trapping of the Nucleus on Micropillared Surfaces Inhibits the Proliferation of Vascular Smooth Muscle Cells but not Cervical Cancer HeLa Cells. *Journal of Biomechanics*, **48**, 1796-1803. https://doi.org/10.1016/j.jbiomech.2015.05.004

[16] Hoorntje, E.T., Bollen, I.A., Barge-Schaapveld, D.Q., van Tienen, F.H., Te Meerman, G.J., Jansweijer, J.A. and van Tintelen, J.P. (2017) *Lamin A/C*-Related Cardiac Disease: Late Onset with a Variable and Mild Phenotype in a Large Cohort of Patients with the Lamin A/C p.(Arg331Gln) Founder Mutation. *Circulation*: *Cardiovascular Genetics*, **10**, e001631. https://doi.org/10.1161/CIRCGENETICS.116.001631

[17] Nagayama, K. and Nishimiya, K. (2020) Moderate Substrate Stiffness Induces Vascular Smooth Muscle Cell Differentiation through Cellular Morphological and Tensional Changes. *Bio-Medical Materials and Engineering*, **31**, 157-167. https://doi.org/10.3233/BME-201087

[18] Hertz, H. (1881) Über die Berührung fester elastischer Körper. *Journal für die reine und angewandte* Mathematik, **92**, 156-171. https://doi.org/10.1515/9783112342404-004

[19] Nagayama, K., Hanzawa, T. and Sato, A. (2023) Superficial Groove Structure in the Size of Focal Adhesion Can Clarify Cell-Type-Specific Differences in Force-Dependent Substrate Mechanosensing. *Journal of Biomechanical Science and Engineering*, **18**, 22-00474. https://doi.org/10.1299/jbse.22-00474

[20] Tseng, Q., Duchemin-Pelletier, E., Deshiere, A., Balland, M., Guillou, H., Filhol, O. and Théry, M. (2012) Spatial Organization of the Extracellular Matrix Regulates Cell-cell Junction Positioning. *Proceedings of the National Academy of Sciences of the United States of America*, **109**, 1506-1511. https://doi.org/10.1073/pnas.1106377109

[21] Butler, J.P., Tolić-Nørrelykke, I.M., Fabry, B. and Fredberg, J.J. (2002) Traction Fields, Moments, and Strain Energy that Cells Exert on Their Surroundings. *American Journal of Physiology*, **282**, 595-605. https://doi.org/10.1152/ajpcell.00270.2001

[22] Nagayama, K. (2019) Biomechanical Analysis of the Mechanical Environment of the Cell Nucleus in Serum Starvation-Induced Vascular Smooth Muscle Cell Differentiation. *Journal of Biomechanical Science and Engineering*, **14**, Article 19-00364. https://doi.org/10.1299/jbse.19-00364

[23] Piludu, M., Piras, M., Pichiri, G., Coni, P., Orrù, G., Cabras, T., Messana, I., Faa, G. and Castagnola, M. (2015) Thymosin Beta 4 May Translocate from the Cytoplasm in to the Nucleus in HepG2 Cells Following Serum Starvation. An Ultrastructural Study. *PLOS ONE*, **10**, e0119642. https://doi.org/10.1371/journal.pone.0119642

[24] Pavlyk, I., Leu, N.A., Vedula, P., Kurosaka, S. and Kashina, A. (2018) Rapid and Dynamic Arginylation of the Leading Edge β-Actin Is Required for Cell Migration. *Traffic*, **19**, 263-272. https://doi.org/10.1111/tra.12551

[25] Nagayama, K., Nogami, K., Sugano, S. and Nakazawa, M. (2024) Dedifferentiation- and Aging-Induced Loss of Mechanical Contractility and Polarity in Vascular Smooth Muscle Cells: Heterogeneous Changes in Macroscopic and Microscopic Behavior of Cells in Serial Passage Culture. *Journal of the Mechanical Behavior of Biomedical Materials*, **160**, 106744. https://doi.org/10.1016/j.jmbbm.2024.106744

[26] Nagayama, K., Nagano, Y., Sato, N. and Matsumoto, T. (2006) Effect of Actin Filament Distribution on Tensile Properties of Smooth Muscle Cells Obtained from Rat thoracic Aortas. *Journal of Biomechanics*, **39**, 293-301. https://doi.org/10.1016/j.jbiomech.2004.11.019

[27] Nagayama, K., Saito, S. and Matsumoto, T. (2015) Multiphasic Stress Relaxation Response of Freshly Isolated and Cultured Vascular Smooth Muscle Cells Measured by Quasi-*in Situ* Tensile Test. *Bio-Medical Materials and Engineering*, **25**, 299-312. https://doi.org/10.3233/BME-151276

[28] Yamashiro, Y., Thang, B.Q., Ramirez, K., Shin, S.J., Kohata, T., Ohata, S., Nguyen, T.A.V., Ohtsuki, S., Nagayama, K. and Yanagisawa, H. (2020) Matrix Mechanotransduction Mediated by Thrombospondin-1/Integrin/YAP Signaling Pathway in the Remodeling of Blood Vessels. *Proceedings of the National Academy of Sciences of the United States of America*, **117**, 9896-9905. https://doi.org/10.1073/pnas.1919702117